Supporting Information for

Effects of Chain Orientation in Self-organized Buffer Layers Based on Poly(3-alkylthiophene)s for Organic Photovoltaics

Fanji Wang[1,2], Kazuhito Hashimoto[2], Hiroshi Segawa[3,4], and Keisuke Tajima[1*]

[1]RIKEN Center for Emergent Matter Science (CEMS), 2-1 Hirosawa, Wako, Saitama 351-0198, Japan, [2]Department of Applied Chemistry Graduate School of Engineering, The University of Tokyo, 7-3-1 Hongo, Bunkyo-ku, Tokyo 113-8656, Japan, [3]Research Center for Advanced Science and Technology, The University of Tokyo, 4-6-1 Komaba, Meguro-ku, Tokyo 153-8904, Japan, and [4]Graduate School of Arts and Sciences, The University of Tokyo, 3-8-1 Komaba, Meguro-ku, Tokyo 153-8902, Japan
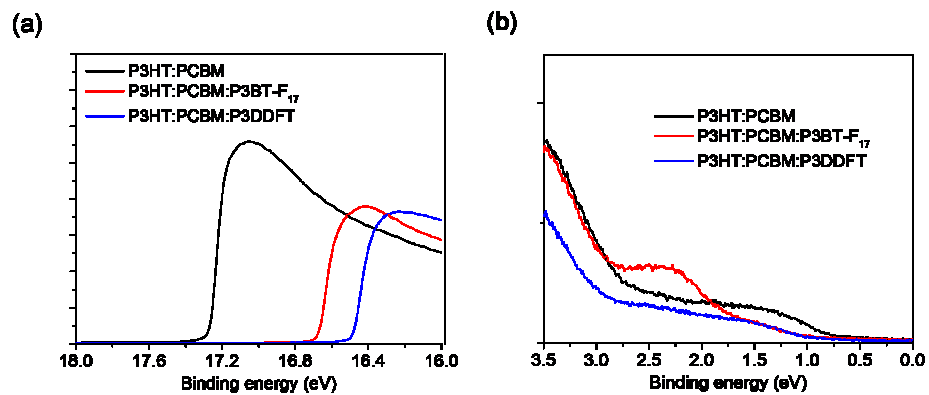
*keisuke.tajima@riken.jp

Figure S1. UPS spectra of P3HT:PCBM (black), P3HT:PCBM:P3BT-F$_{17}$ (red), and P3HT:PCBM:P3DDFT (blue) films in the (a) cutoff regions and (b) Fermi-edge regions. The samples were irradiated using He(I) with a photon energy of 21.2 eV.
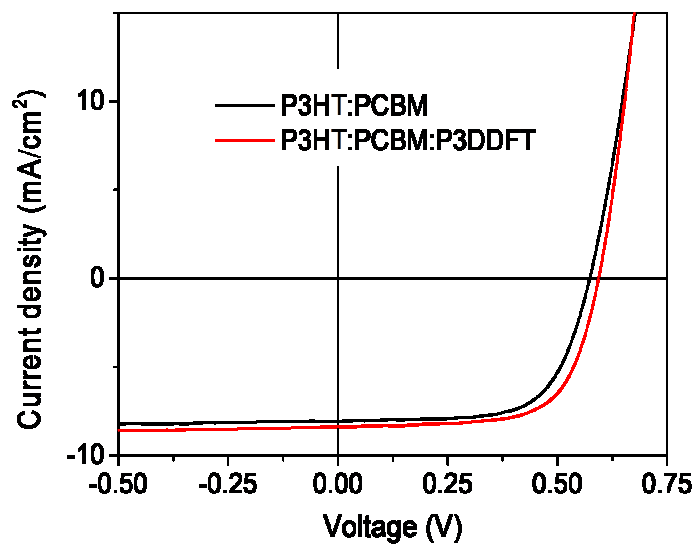
Figure S2. *J–V* curves under simulated solar irradiation (AM 1.5, 100 mW cm^{-2}) for bulk heterojunction OPV devices based on P3HT:PCBM spin coated from CB with (red) or without (black) the self-organized buffer layer of P3DDFT.
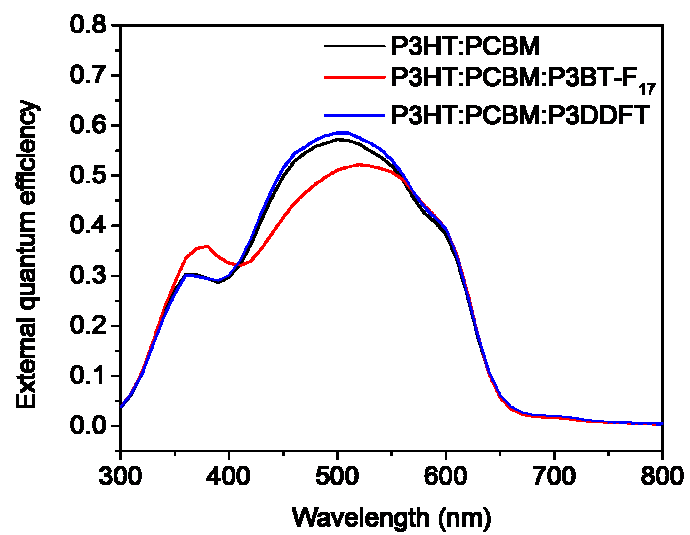
Figure S3. EQE spectra for OPVs with the active layers of P3HT:PCBM (black),

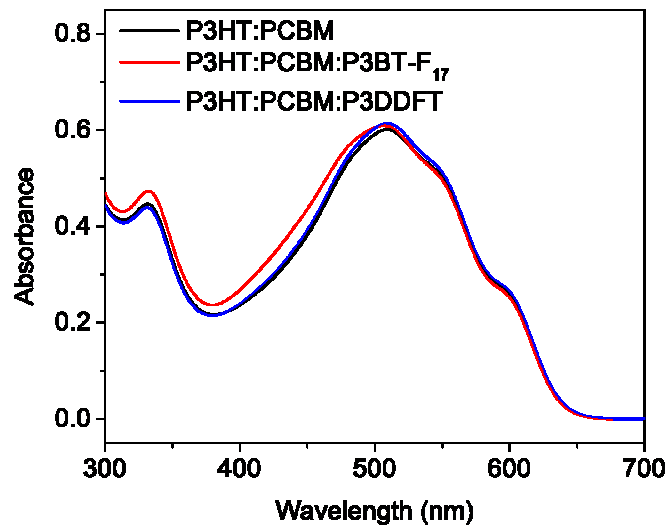P3HT:PCBM:P3BT-F$_{17}$ (red), and P3HT:PCBM:P3DDFT (blue).

Figure S4. UV–vis absorption spectra in transmittance mode for films of P3HT:PCBM (black), P3HT:PCBM:P3BT-F$_{17}$ (red), and P3HT:PCBM:P3DDFT (blue).
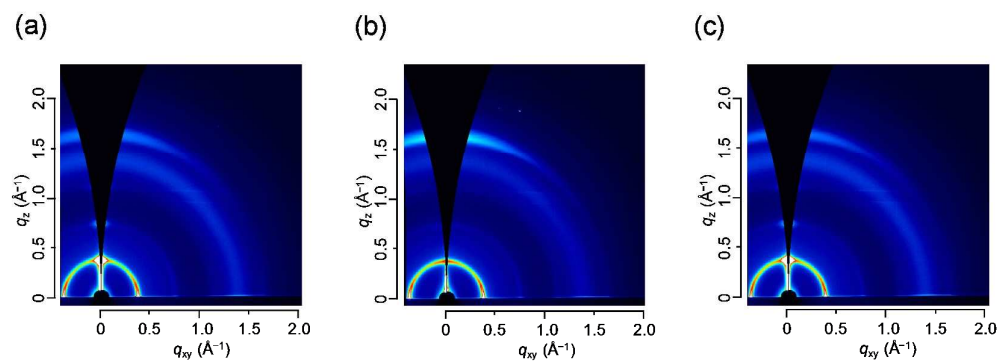
Figure S5. 2D GIWAXS patterns for films of (a) P3HT:PCBM and (b) P3HT:PCBM:P3BT-F$_{17}$ and (c) P3HT:PCBM:P3DDFT
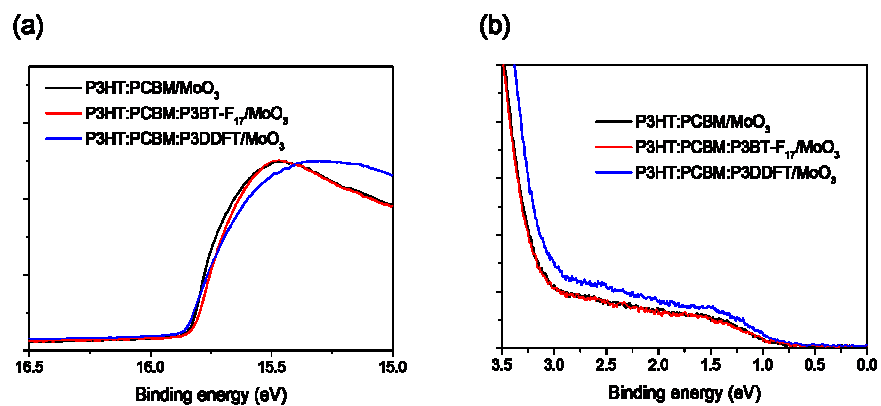
Figure S6. UPS spectra of P3HT:PCBM/MoO$_3$ (black), P3HT:PCBM:P3BT-F$_{17}$/MoO$_3$ (red), and P3HT:PCBM:P3DDFT/MoO$_3$ (blue) films in (a) cutoff region and (b) Fermi-edge region. The samples were irradiated using He(I) with a photon energy of 21.2 eV.
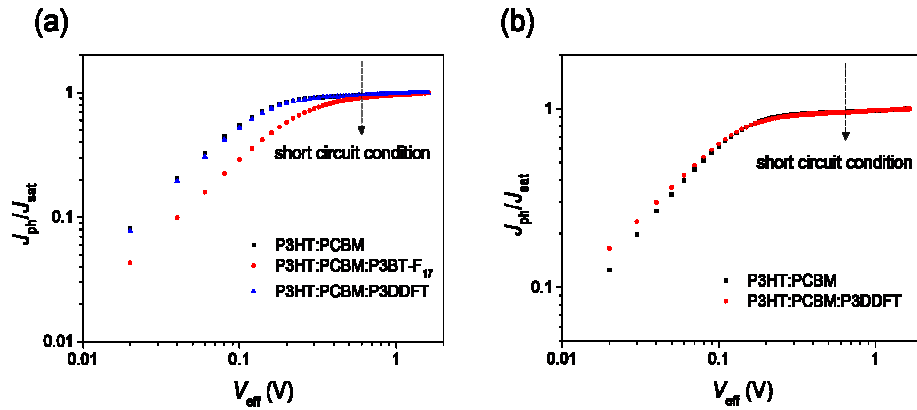
Figure S7. Normalized photocurrent density (J_{ph}/J_{sat}) plotted against effective voltage (V_{eff}) in the cells with active layers prepared by (a) CHCl$_3$ and (b) CB. The short circuit conditions are indicated by dashed arrows.

Estimation of the charge separation probability at short circuit condition

To show the difference and the similarity in the photogeneration ability among the three OPVs more clearly, we have analyzed normalized photocurrent density (J_{ph}/J_{sat}) plotted against effective voltage (V_{eff}). Photocurrent (J_{ph}) is defined as $J_{light}-J_{dark}$, in which J_{light} and J_{dark} are the current density under AM1.5 and dark, respectively. J_{sat} is the maximum current density based on the assumption that all the photogenerated bound pairs at charge transfer state (CTS) could dissociate into free charges, transport to the electrode and contribute to the photocurrent. (Blom et al, *Phys. Rev. Lett.* **2004**, *93*, 216601. and Chen et.al, *ACS Nano* **2011**, *5*, 959-967.) The V_{eff} is calculated as $V_0-V_{applied}$, where V_0 is voltage with zero photocurrent and $V_{applied}$ is externally applied voltage. Therefore, by normalizing the photocurrent with respect to J_{sat} of each devices, we could compare the charge separation probability of three devices at short circuit condition. The values were 95.1%, 91.7% and 94.9% for P3HT:PCBM, P3HT:PCBM:P3BT-F$_{17}$ and P3HT:PCBM:P3DDFT devices, respectively, when prepared from CHCl$_3$ solutions (Figure S7a) and 96.5% and 96.1% for P3HT:PCBM and P3HT:PCBM:P3DDFT devices, respectively, when prepared from CB solutions

(Figure S7b). The similar charge separation probability between P3HT:PCBM and P3HT:PCBM:P3DDFT devices suggest the comaprable charge separation efficiency, which implys similar mixed morphology. Nevertherless, a higher J_{sc} was observed for P3HT:PCBM:P3DDFT device, which can be attributed to the efficient hole extraction at the electrode interface induced by the SSM. In contrast, P3HT:PCBM:P3BT-F$_{17}$ device showed the lowest charge separation probability, which could reflect the change in the mixed morphology induced by P3BT-F$_{17}$ on the surface.